AD-A112 781 OHIO STATE UNIV COLUMBUS ELECTROSCIENCE LAB F/G 20/14
CURVED SURFACE MOUNTED ANTENNA RADIATING IN THE PRESENCE OF PER--ETC(U)
MAY 81 R ROJAS, W D BURNSIDE N00019-80-C-0050
UNCLASSIFIED ESL-712527-3 NL

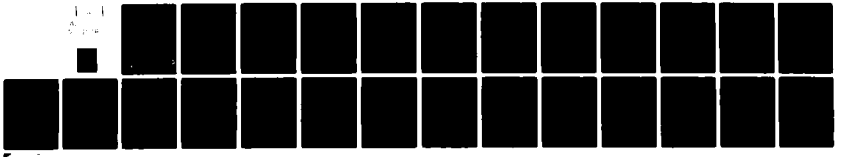

END
DATE FILMED
4 82
DTIC

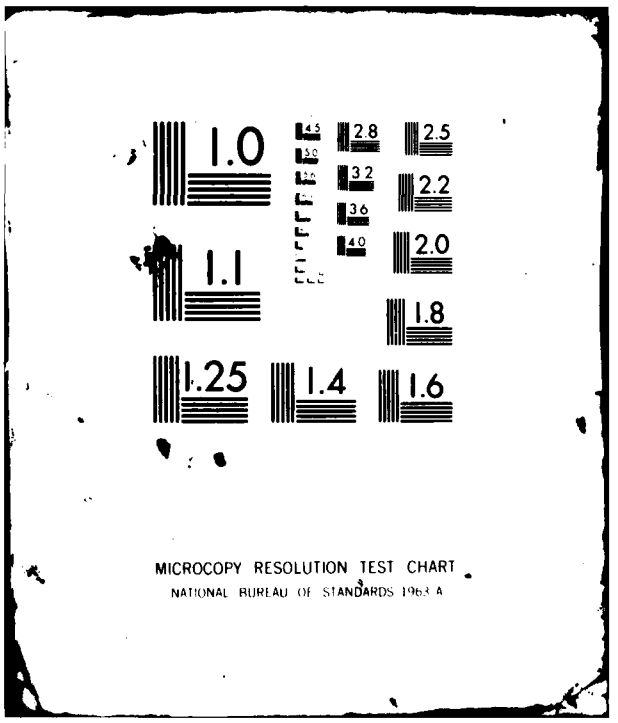
1.0
1.1
1.25
1.4
1.6
2.8
3.2
3.6
4.0
2.5
2.2
2.0
1.8
MICROCOPY RESOLUTION TEST CHART
NATIONAL BUREAU OF STANDARDS 1963 A

OSU

The Ohio State University

CURVED SURFACE MOUNTED ANTENNA RADIATING IN THE PRESENCE OF PERFECTLY CONDUCTING PLATES

R. Rojas
and
W.D. Burnside

The Ohio State University

ElectroScience Laboratory

Department of Electrical Engineering
Columbus, Ohio 43212

Technical Report 712527-3
Contract No. [redacted]
May 1981

Department of the Navy
Naval Air Systems Command
Washington, D.C. 20361

NOTICES

When Government drawings, specifications, or other data are used for any purpose other than in connection with a definitely related Government procurement operation, the United States Government thereby incurs no responsibility nor any obligation whatsoever, and the fact that the Government may have formulated, furnished, or in any way supplied the said drawings, specifications, or other data, is not to be regarded by implication or otherwise as in any manner licensing the holder or any other person or corporation, or conveying any rights or permission to manufacture, use, or sell any patented invention that may in any way be related thereto.

Unclassified

SECURITY CLASSIFICATION OF THIS PAGE (When Data Entered)

REPORT DOCUMENTATION PAGE	READ INSTRUCTIONS BEFORE COMPLETING FORM
1. REPORT NUMBER	2. GOVT ACCESSION NO. AD-A112 781 / 3. RECIPIENT'S CATALOG NUMBER
4. TITLE (and Subtitle) CURVED SURFACE MOUNTED ANTENNA RADIATING IN THE PRESENCE OF PERFECTLY CONDUCTING PLATES	5. TYPE OF REPORT & PERIOD COVERED Technical 6. PERFORMING ORG. REPORT NUMBER ESL 712527-3
7. AUTHOR(s) R. Rojas and W.D. Burnside	8. CONTRACT OR GRANT NUMBER(s) N00019-80-C-0050
9. PERFORMING ORGANIZATION NAME AND ADDRESS The Ohio State University ElectroScience Laboratory, Department of Electrical Engineering, Columbus, Ohio 43212	10. PROGRAM ELEMENT, PROJECT, TASK AREA & WORK UNIT NUMBERS
11. CONTROLLING OFFICE NAME AND ADDRESS Department of the Navy Naval Air Systems Command Washington, D.C. 20361	12. REPORT DATE May 1981 13. NUMBER OF PAGES 20
14. MONITORING AGENCY NAME & ADDRESS(if different from Controlling Office)	15. SECURITY CLASS. (of this report) Unclassified 15a. DECLASSIFICATION/DOWNGRADING SCHEDULE

16. DISTRIBUTION STATEMENT (of this Report)

APPROVED FOR PUBLIC RELEASE
DISTRIBUTION UNLIMITED

17. DISTRIBUTION STATEMENT (of the abstract entered in Block 20, if different from Report)

18. SUPPLEMENTARY NOTES

19. KEY WORDS (Continue on reverse side if necessary and identify by block number)

Electromagnetic radiation
High frequency solutions
Geometrical Theory of Diffraction
Far field patterns
Near field patterns
Prolate spheroid mounted antenna
Flat plate scatterer
Pattern distortion effects
Measured versus calculated results

20. ABSTRACT (Continue on reverse side if necessary and identify by block number)

A method for computing the patterns of monopole or aperture antennas mounted on a perfectly conducting convex surface radiating in the presence of a metal plate is presented. The Geometrical Theory of Diffraction (GTD) is used to analyze the radiating system. Systematic methods for computing the individual components of the total high-frequency field are discussed. The receiver location can range from a wavelength away from any structure to the far-zone. The accuracy of the solutions is demonstrated by comparisons with measured results, where a $2\lambda \times 4\lambda$ prolate spheroid is used as the convex surface.

DD FORM 1 JAN 73 1473 EDITION OF 1 NOV 65 IS OBSOLETE

Unclassified

SECURITY CLASSIFICATION OF THIS PAGE (When Data Entered)

TABLE OF CONTENTS

LIST OF FIGURES

I. Radiation Pattern of Antennas Mounted on a Perfectly Conducting Convex Body

There is a great deal of interest in calculating the patterns of antennas radiating in the presence of complex structures such as an aircraft, ship, etc. One of the approaches that has found great success for analyzing these types of problems is the Geometrical Theory of Diffraction (GTD). Probably the biggest advantage of this method over others is that many electrically large structures can be modeled using flat plates, and some kind of convex body such as a cylinder, sphere, spheroid, etc., for which diffraction coefficients are known.

The radiating system shown in Figure 1 is a good starting point in solving more complicated structures, because it illustrates most of the individual field components making up the total high-frequency radiated field. As depicted in Figure 1, let us consider an antenna mounted on a perfectly conducting convex surface in the presence of an n-sided, (n=4 in Figure 1) finite perfectly conducting plate. In order to avoid some geometric complications, let us assume that the plate is not attached to the convex surface. The total field at the point (p), which has to be at least a wavelength away from any diffraction point is equal to the superposition of the following field components as shown in Figure 2.

(1) direct field from the source
(2) reflected fields from the finite metal plate.
(3) curved surface diffracted fields from the convex surface
(4) diffracted fields from the edges of the plate.
(5) vertex diffraction from each of the plate corners.

Let us consider two types of antennas: slots and monopoles. The length (L) of the monopole can not exceed a quarter of a wavelength,

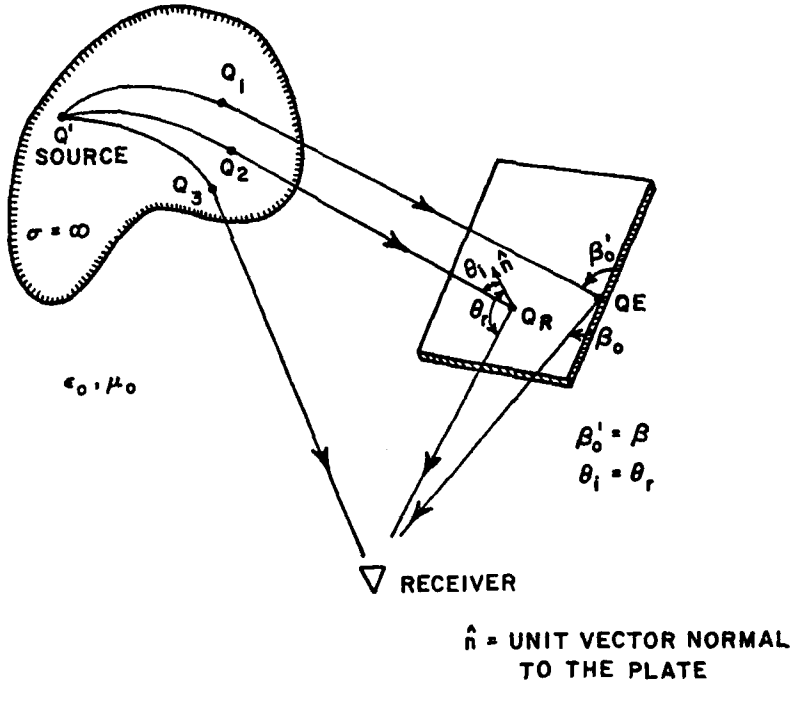

Figure 1. Curved surface mounted antenna radiating in the presence of a metal plate.

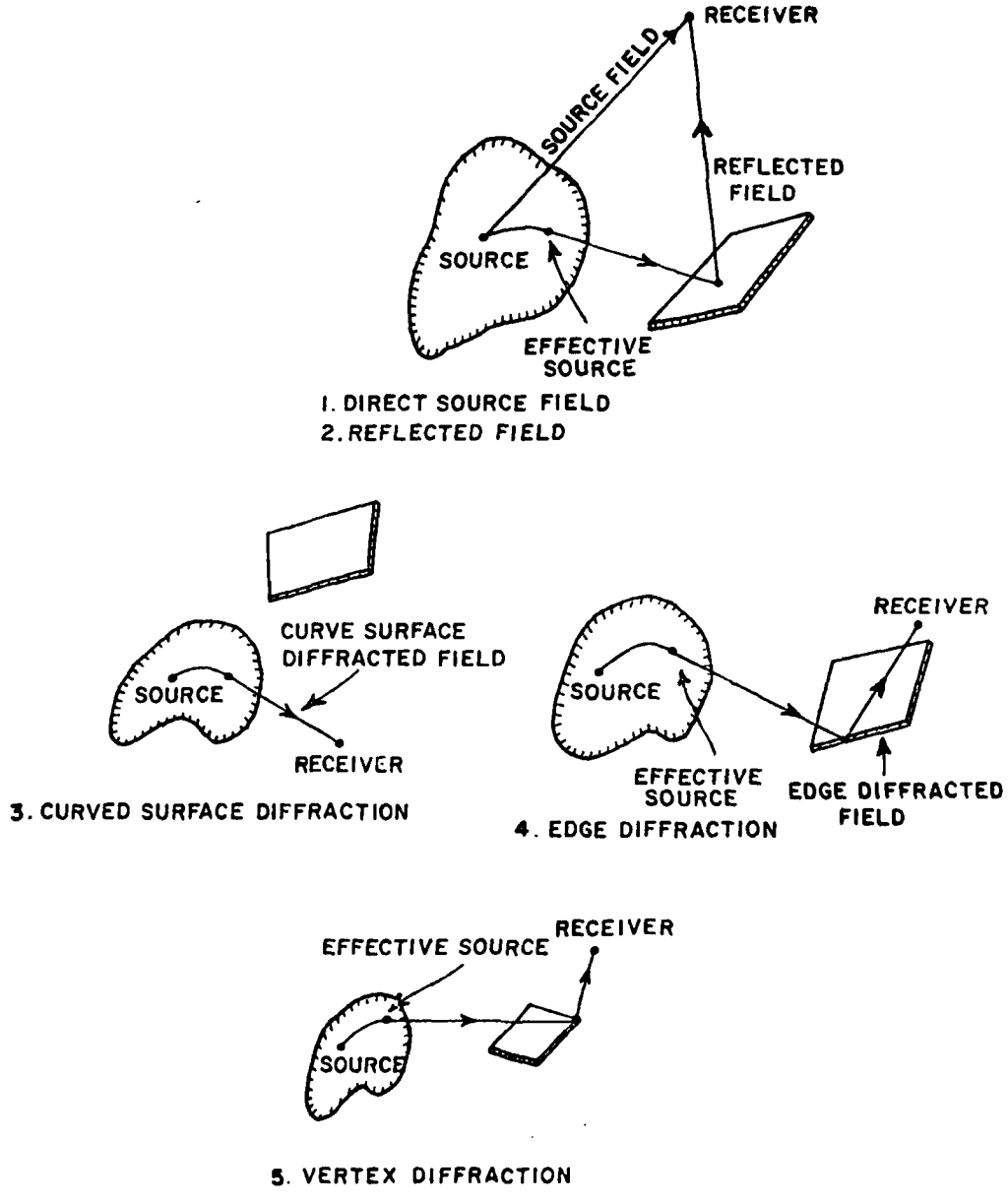

Figure 2. Various terms used in calculating the total high-frequency field.

and for the slot antenna it is assumed that a cosine field distribution exists along the magnetic dipole axis, and a uniform distribution across the dipole axis. These restrictions are necessary because of the nature of the approximations made in obtaining the high-frequency fields. References [1]and [2] describe these approximations in detail.

The first step in the solution of each term of the total GTD field is to determine the ray path using the laws of reflection and/or diffraction. Assuming the ray path is determined, one must then examine the total ray path to see whether or not it intersects an obstacle. If the ray path is not interrupted, the field value is computed and superimposed with other terms. On the other hand, if the path is interrupted, the field is not computed.

A. Source Field

The direct and curved surface diffracted fields are computed using the results given in [3]. Both fields will be referred to as the source fields in the rest of this report. Obviously, when the field point is in the lit region, the lit region solution is used; whereas, the shadow region solution is used if the field point is in the shadow region.

B. Reflected Field

In order to determine the path of the reflected field from the plate, the receiver image position is found as illustrated in Figure 3. The source solution is then used to compute the $\overline{E^s}$ field at the image position. The second step is to ascertain if the ray path from the effective source to the image position intersects the plate. If it does intersect, the reflected field $\overline{E^r}$ at (x_r, y_r, z_r) is computed as follows

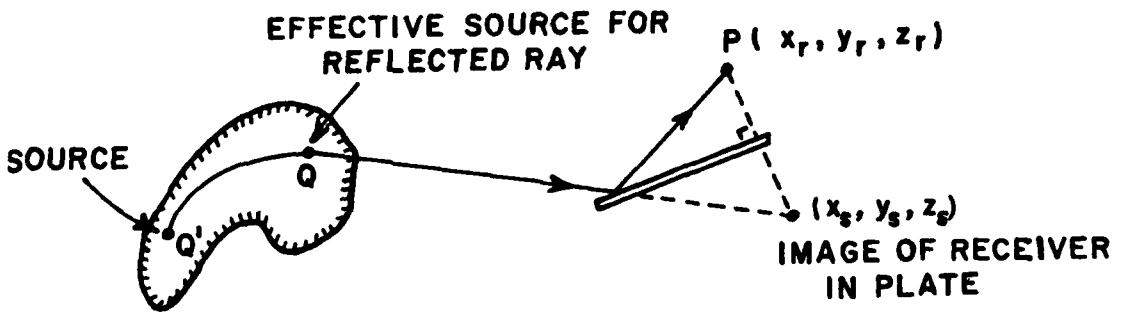

Figure 3. Geometry used to determine reflected field from metal plate.

$$\begin{bmatrix} E_x^r \\ E_y^r \\ E_z^r \end{bmatrix} = \begin{bmatrix} T_{xx} & T_{xy} & T_{xz} \\ T_{yx} & T_{yy} & T_{yz} \\ T_{zx} & T_{zy} & T_{zz} \end{bmatrix} \begin{bmatrix} E_x^s \\ E_y^s \\ E_z^s \end{bmatrix} , \qquad (1)$$

where $E^s = E_x^s \hat{x} + E_y^s \hat{y} + E_z^s \hat{z}$ is the source field incident on the image receiver position.

If the ray path is not interrupted by the plate, the reflected field is not computed. The T-matrix in equation (1) represents the reflected field polarization transformation matrix. It is derived in detail in [2]. It turns out that the T-matrix elements are independent of the receiver location. Thus, in order to improve the efficiency of the numerical solution, the T-matrix is stored in memory.

C. Edge-Diffracted Field

The diffracted fields from the edges of the plate are obtained using the diffraction coefficients presented in [4]. Assuming that one has determined the ray paths for these fields, the diffracted fields are given by

$$\bar{E}^d(s) = \bar{E}^i(Q_E) \cdot \bar{\bar{D}}(\phi,\phi';\beta_0') \sqrt{\frac{\rho}{s(\rho+s)}}\, e^{-jks} , \qquad (2)$$

where

$$\bar{\bar{D}}(\phi,\phi';\beta_0') = -\hat{\beta}_0' \hat{\beta}_0 D_s(\phi,\phi';\beta_0') - \hat{\phi}'\hat{\phi} D_h(\phi,\phi';\beta_0') , \qquad (3)$$

where D_s is the scalar diffraction coefficient for the acoustically soft (Dirichlet) boundary condition at the surface of the plate, and D_h is the scalar diffraction coefficient for the acoustically hard (Neumann) boundary condition. Expressions for D_s and D_h are given in [4]. $\bar{E}^i(Q_E)$, the source field incident on the edges of the plate can be determined from the expressions for the source field.

The edge diffraction coefficients were obtained for infinite straight edges, and since the plate is finite, there will be a discontinuity in the edge diffracted fields due to the corners of the plate. To compensate for this discontinuity, a diffraction coefficient associated with the corners of the plate is needed. Expressions for the corner diffracted fields associated with one corner on one edge are given in [5]. It is enough to mention that this coefficient in its present form predicts accurately the corner effect of various plate structures.

Probably the most difficult part in computing the edge diffracted field is to determine the ray path. As depicted in Figure 4, the law of diffraction ($\hat{s}' \cdot \hat{e} = \hat{s} \cdot \hat{e}$) is used to find the point of diffraction (x_d, y_d, z_d). For any particular source, plate edge, and receiver location, the diffracted ray path is unique. The key in finding this unique path is to determine the diffraction point along a given edge of the plate. Efficient algorithms to calculate the diffraction point have been developed at the ElectroScience Laboratory. These algorithms can calculate the diffraction point for any edge, including the junction edge (the edge formed by the junction of the plate and convex surface). The junction edge need not be straight, which complicates the solutions. For a complete description of the algorithms refer to [2] or [6].

II. Results

The geometry used to test the validity of the analytical solutions is illustrated in Figure 5, where two cartesian coordinate systems are defined. One of them is the cartesian system ($\hat{x}', \hat{y}', \hat{z}'$) which defines the spheroid and plate geometries. This system is then rotated into what is referred to as the ($\hat{x}, \hat{y}, \hat{z}$) system. Note that the new coordinate system is found by first rotating about the z' axis the angle ϕ_c, and then about the y-axis the angle θ_c. The conical pattern

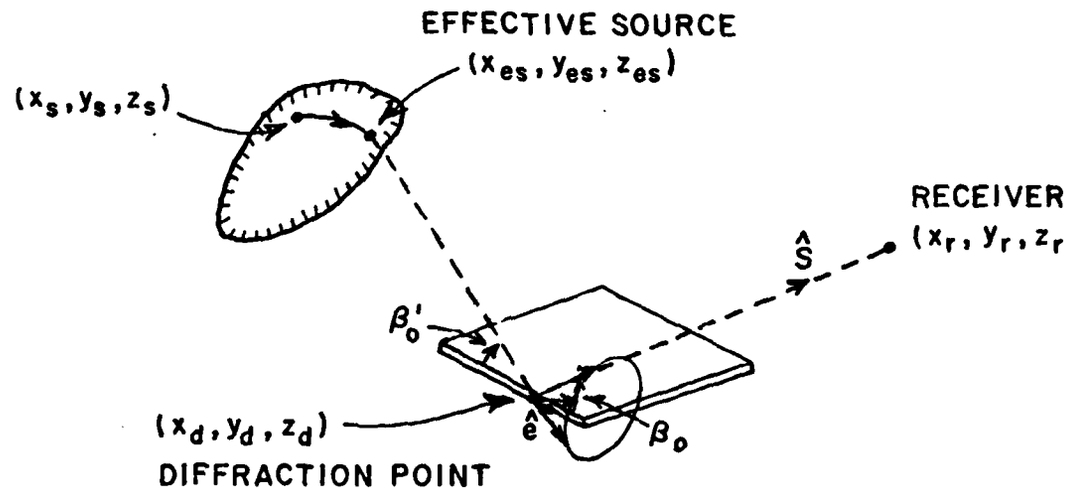

Figure 4. Geometry depicting diffraction from straight edge of metal plate.

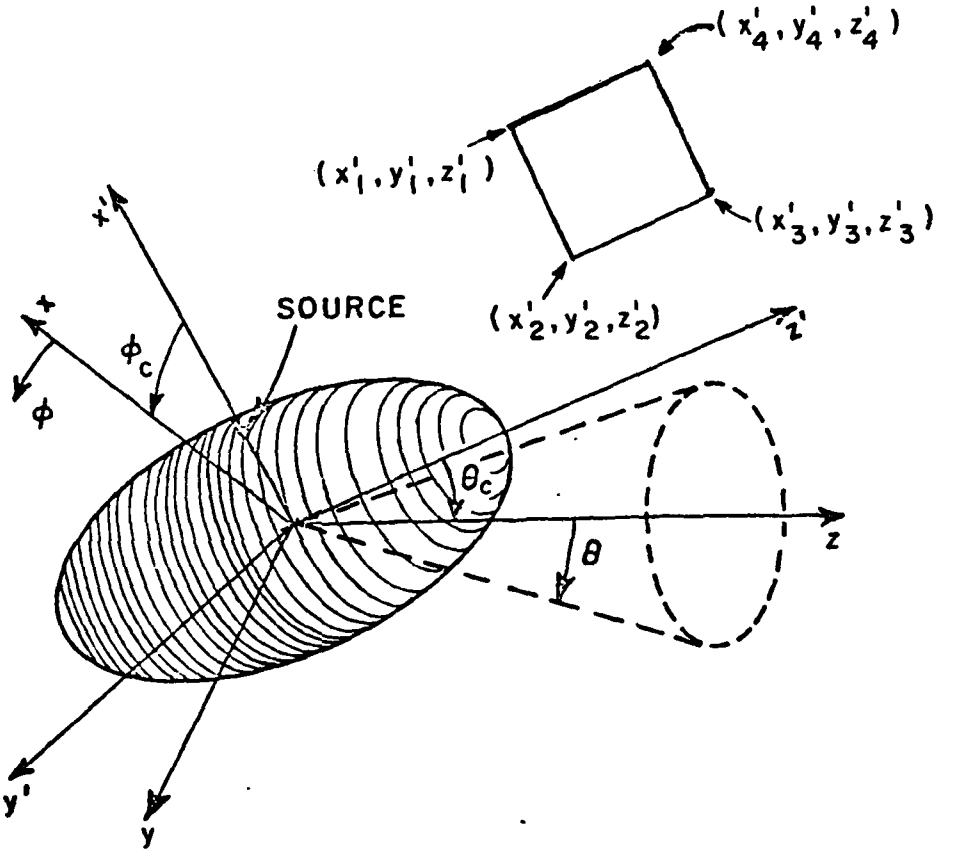

Figure 5. Coordinate systems used to define the spheroid and plate geometries and the pattern axis.

is then taken in the $(\hat{x}, \hat{y}, \hat{z})$ system with θ fixed and varying ϕ from 0^{o} to 360^{o}.

Calculated and measured roll-plane patterns ($\theta_c = 0^{o}$., $\phi_c = 0^{o}$., $\theta = 90^{o}$.) are shown in Figure 6 for a quarter inch monopole antenna located at $\theta_s = 90^{o}$ radiating without the presence of the plate. Both results agree very well except in the region from $\phi = 144^{o}$ to $\phi = 216^{o}$, where the calculated results are a few decibels below the measured pattern. This is due to the fact that only 2 surface rays (rays 1 and 2) shown in Figure 7 are used. Because of the dimensions of the spheroid, i.e., $c = 4\lambda$ is only twice as long as $a = 2\lambda$, the contributions of rays 3 and 4 are important, and if included, the calculated pattern would resemble more closely the measured results. In all the results presented here, only 2 surface rays are used. Figures 8 and 9 illustrate two roll-plane patterns for a quarter inch monopole radiating in the presence of a 10" x 10" metal plate. There is a very good agreement between the calculated and measured patterns, even though, in making the measurements it was very difficult to position the plate at the desired location due to the lack of a reference coordinate system.

Figure 10 shows the geometry used to calculate the patterns depicted in Figures 11, 12, and 13. As indicated before, the total high frequency field is equal to the superposition of individual terms. Figure 11 illustrates the individual source, reflected, and diffracted fields together with the total field for a roll-plane cut ($\theta_c = 0^{o}$., $\phi_c = 0^{o}$., $\theta = 90^{o}$.) Figure 12 shows the effect of adding the corner diffracted term to the total solution, and it is clear that the discontinuity around $\phi = 70^{o}$ is removed when the corner diffracted term is added. The conical patterns are for $\theta_c = 0^{o}$., $\phi_c = 0^{o}$., $\theta = 75.1^{o}$. Finally, Figure 13 illustrates patterns for axial and circumferential 0.4" x 0.8" slots located at $\theta_s = 90^{o}$.

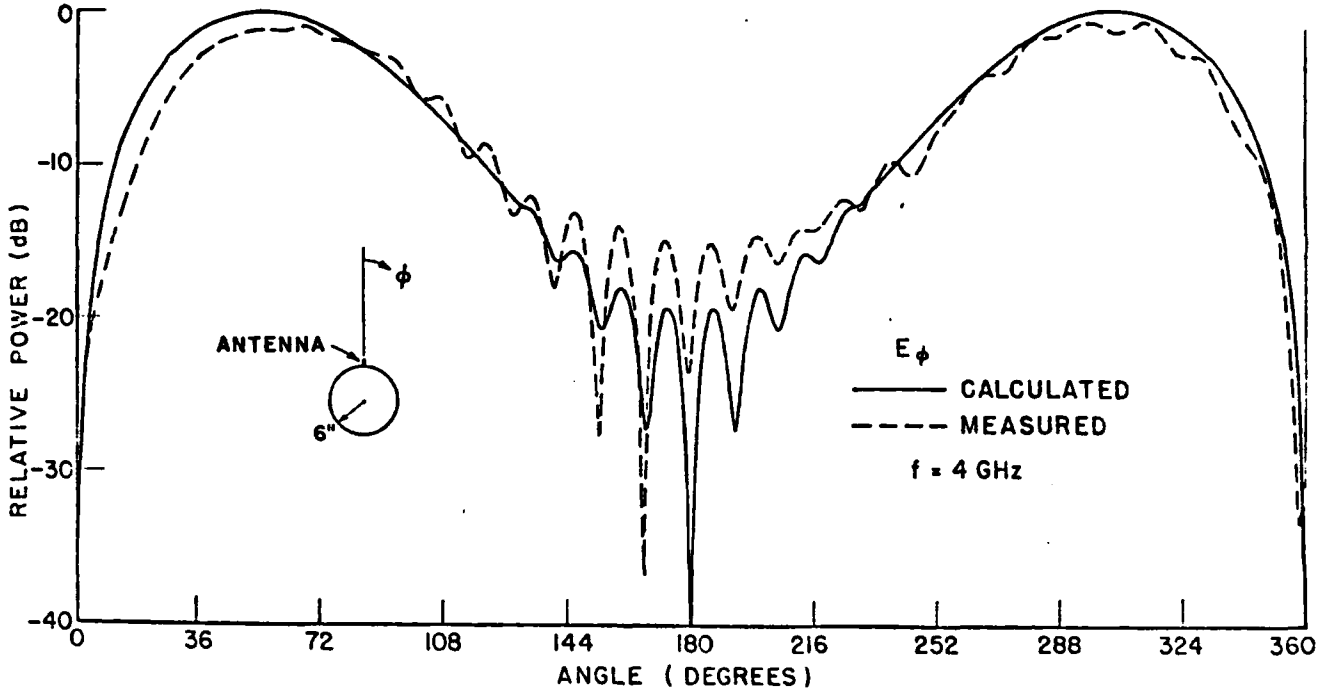

Figure 6. Roll plane (θ_c=0, ϕ_c=0, θ=90) patterns for a 0.25" monopole mounted at θ_s=90. Only rays 1 and 2 are included (see Figure 7).

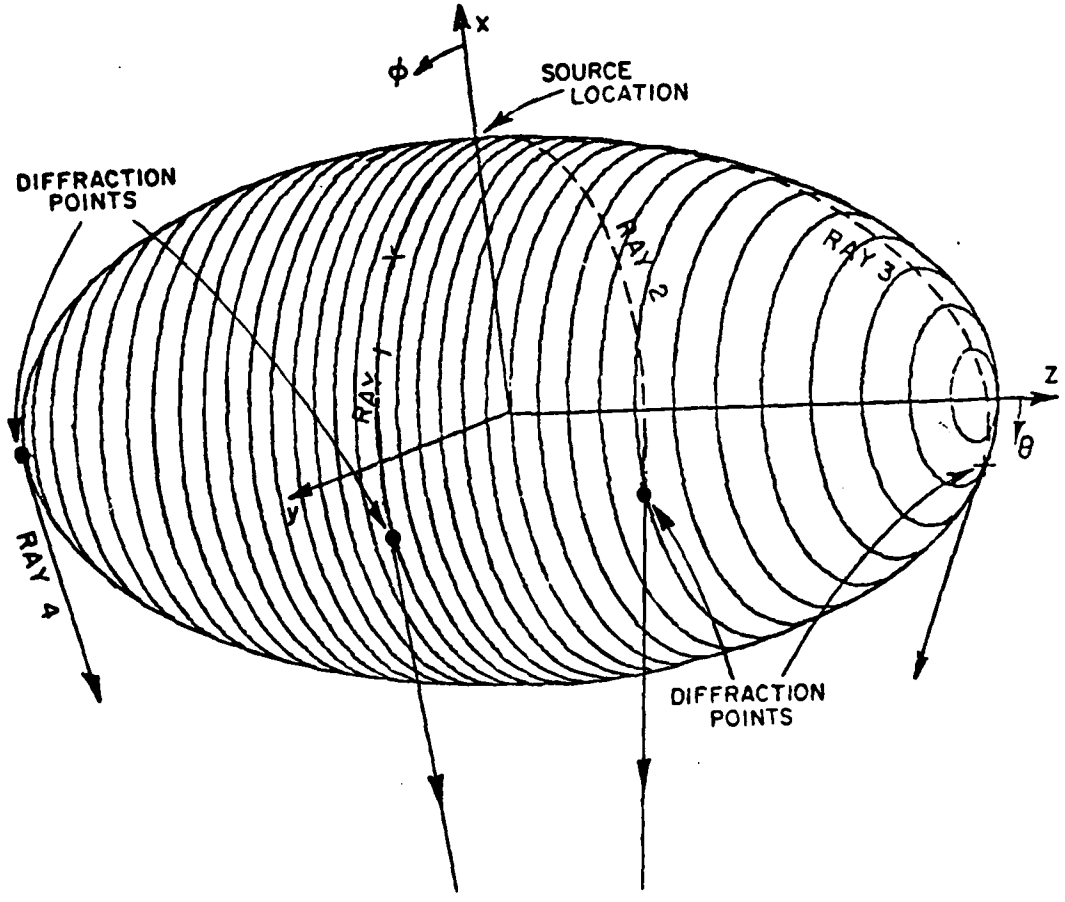

Figure 7. The four dominant GTD terms that radiate at (θ=90°, ϕ=180°).

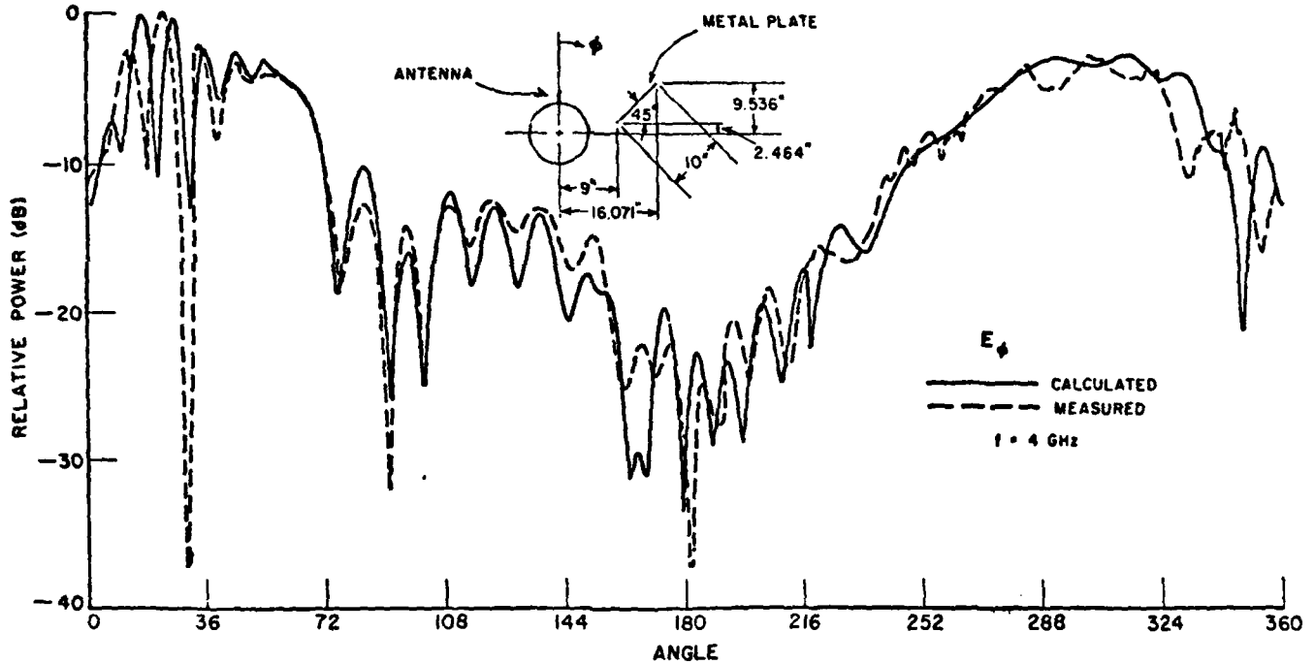

Figure 8. Roll plane ($\theta_c=0^o$, $\phi_c=0^o$, $\theta=90^o$) patterns for a 0.25" monopole mounted at $\theta_s=90^o$ on a 2λ x 4λ spheroid.

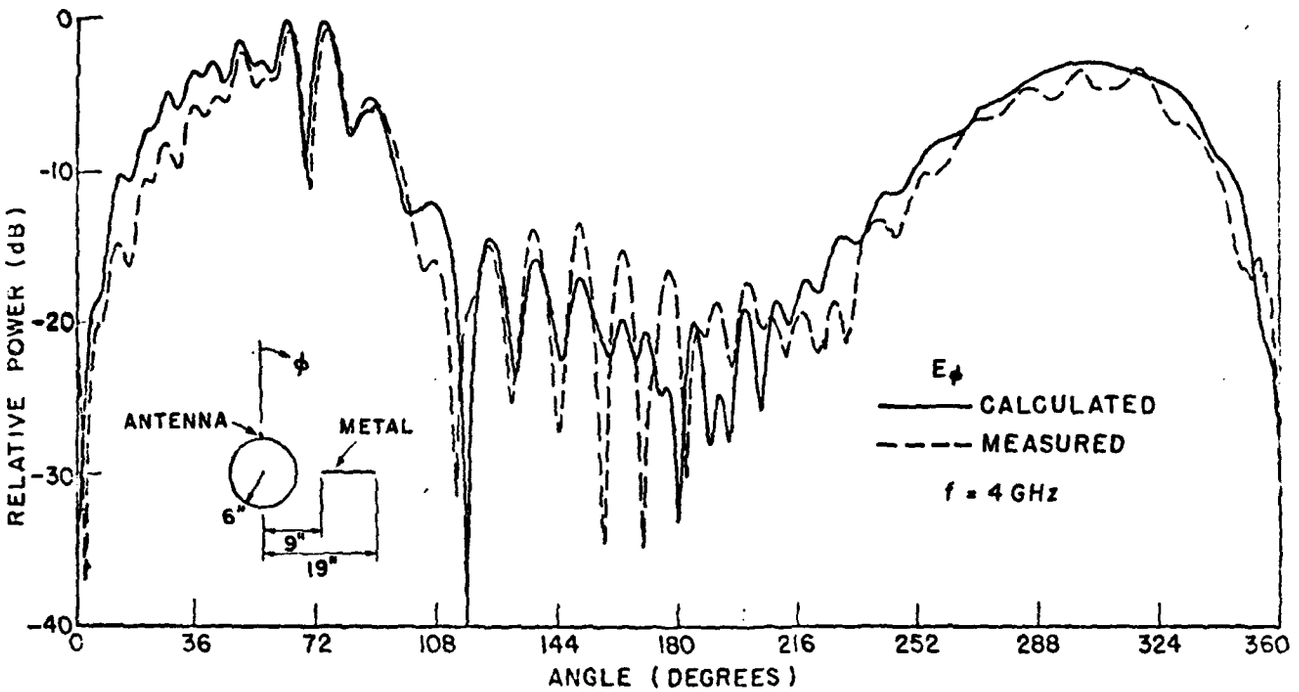

Figure 9. Roll plane ($\theta_c=0^o$, $\phi_c=0^o$, $\theta=90^o$) patterns for a 0.25" monopole mounted at $\theta_s=90^o$ on a 2λ x 4λ spheroid.

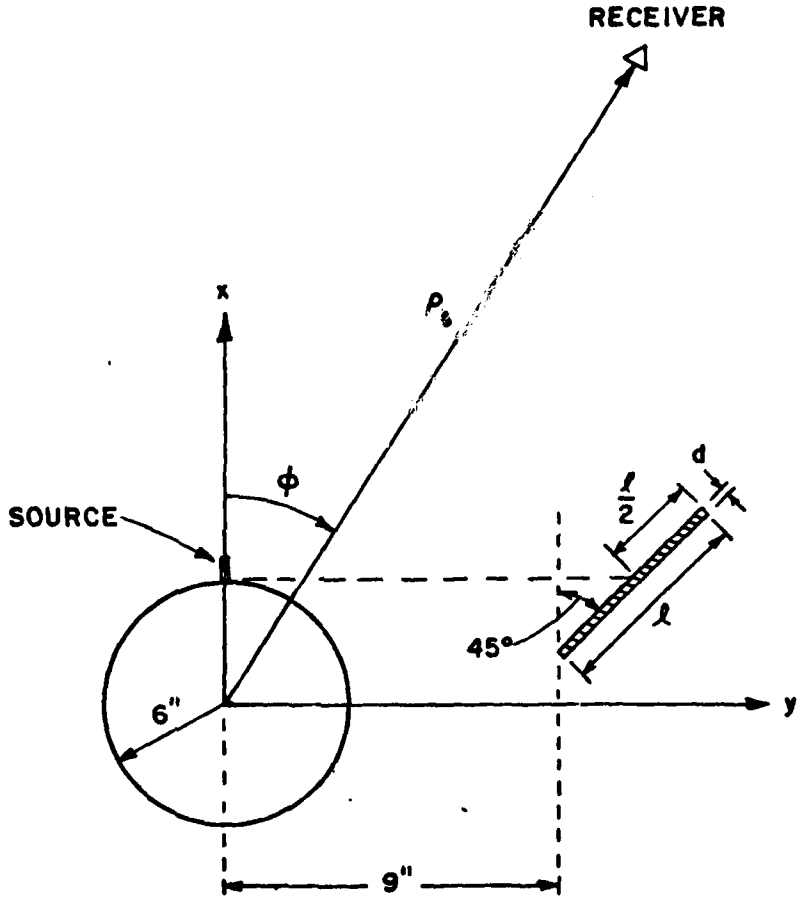

Figure 10. End view of the geometry used to calculate the conical patterns depicted in Figures 11-13.

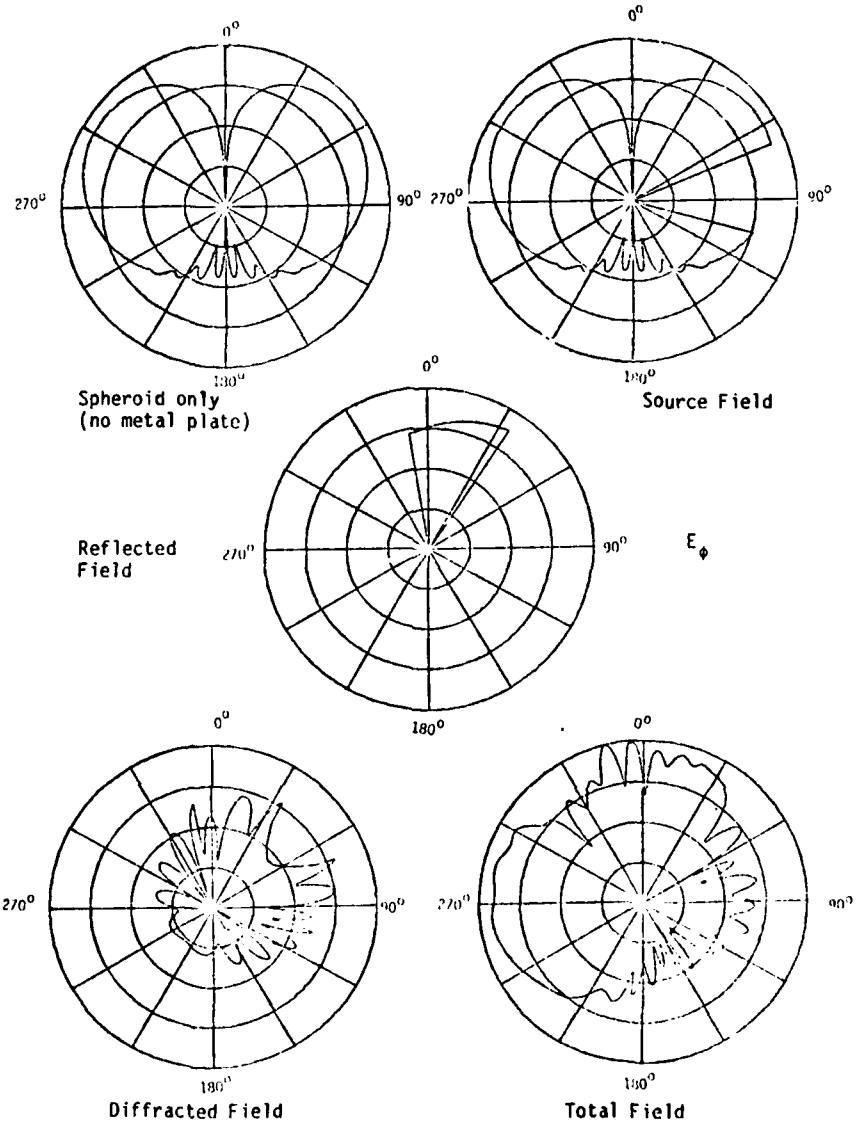

Figure 11. Calculated radiation patterns (θ_c=0°, ϕ_c=0°, θ=90°) for a 0.25" monopole mounted at θ_s=90°. The metal plate is a 10" x 10" square.

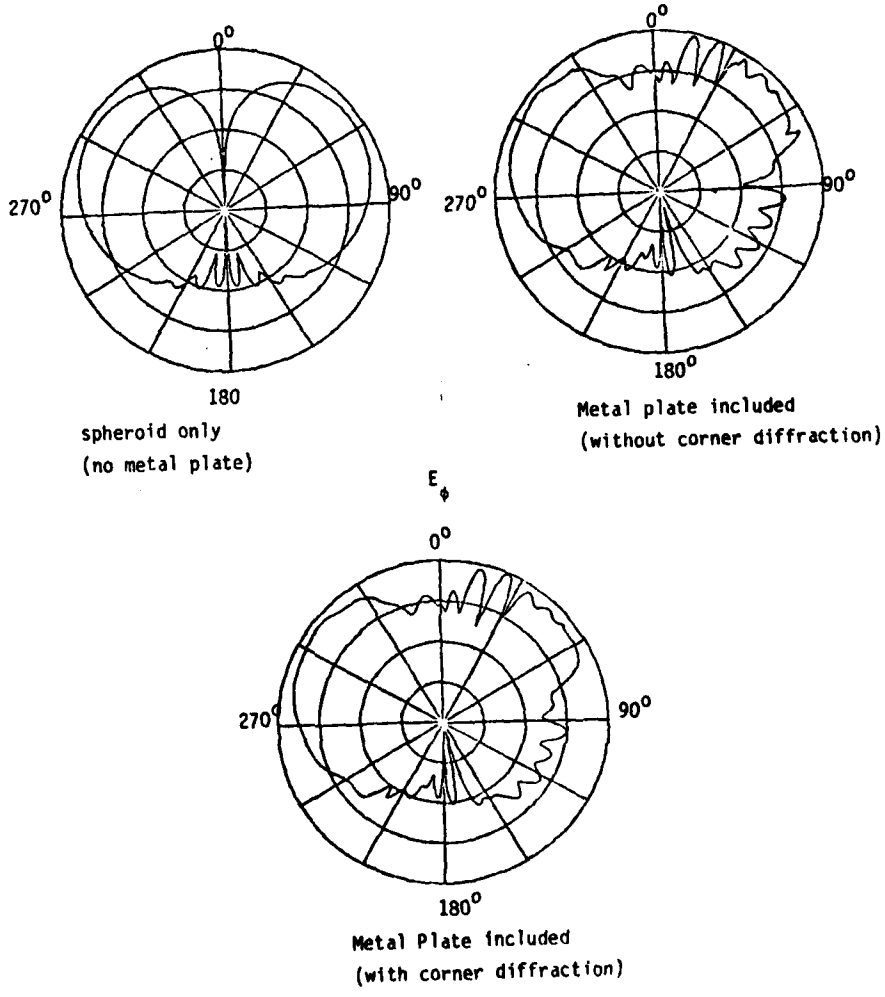

Figure 12. Calculated patterns (θ_c=0°, ϕ_c=0°, θ=75.10°) for a 0.25" monopole located at θ_s=90°. The metal plate is a 10"x10" square.

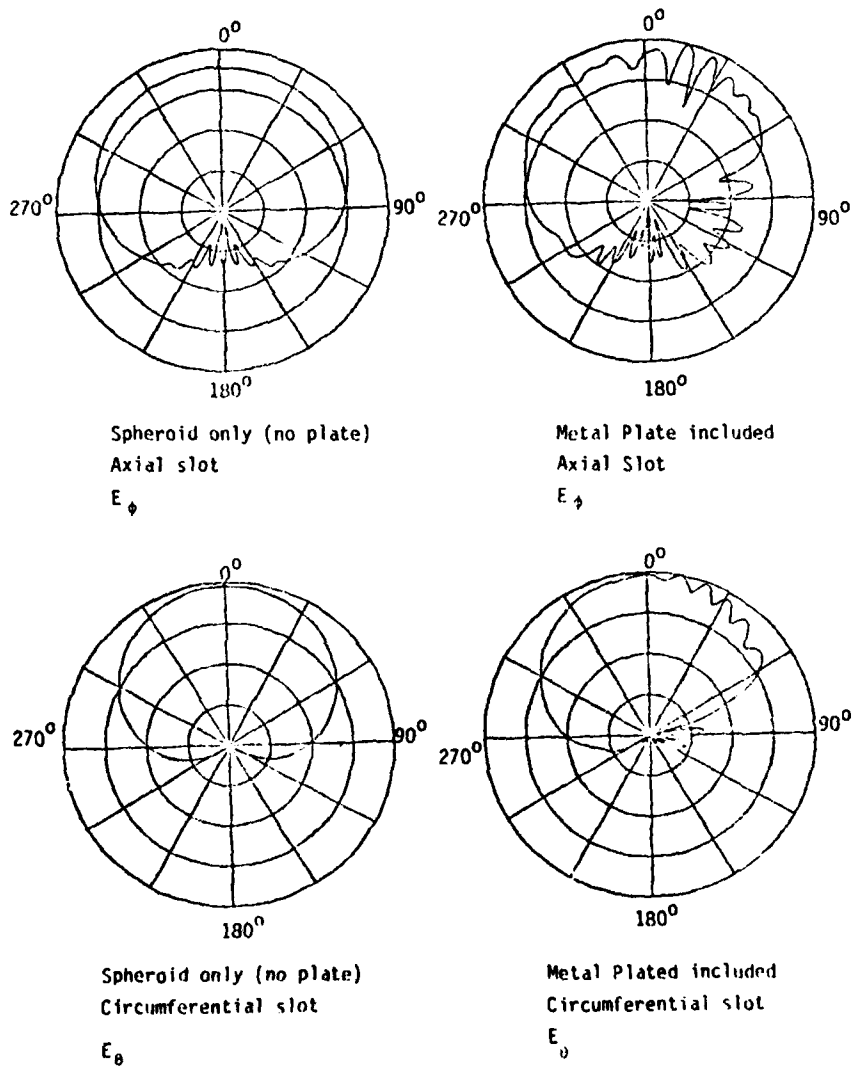

Figure 13. Calculated roll-plane ($\theta_c=0^o$, $\phi_c=0^o$, $\theta=90^o$) patterns for a 0.4"x0.8" slot located at $\theta_s=90^o$. The metal plate is a 10"x10" square.

A very important property of GTD was illustrated when the corner diffracted term was added in Figure 12. If any term that is significant in the total solution is not included, it shows up in the calculated pattern in the form of a jump or a kink. Thus, one has an automatic check on the results and can correct for errors by adding higher order terms to the solution until a continuous pattern is obtained.

It is important to emphasize that all the results presented above were obtained for a very stringent case due to the dimensions of the spheroid, which is approaching a sphere. To actually model a missile, or aircraft fuselage, the electric dimensions of the spheroid would be much larger than the ones chosen here, i.e., $2\lambda \times 4\lambda$. Since GTD is based on the assumption of the locality of the diffraction phenomenon, one should expect to obtain more accurate calculated patterns when the spheroid is larger in terms of wavelength.

REFERENCES

1. N. Wang, "Near Field Solutions for Antennas on Elliptic Cylinder," The Ohio State University ElectroScience Lab., Dept. of Electrical Engineering; prepared under contract N00019-77-C-0299 for the Naval Air Systems Command, Report 784685-1, July 1977.

2. W.D. Burnside, N. Wang, and E.L. Pelton, "Near Field Pattern Computations for Airborne Antennas," IEEE Trans., Vol. AP-28, pp. 318-327, May 1980.

3. C.C. Huang, N. Wang, and W.D. Burnside, "The High Frequency Radiation Patterns of a Spheroid-Mounted Antenna," The Ohio State University ElectroScience Lab., Department of Electrical Engineering; prepared under Contract N00019-80-C-0050 for Naval Air Systems Command, Report 712527-1, March 1980.

4. R.G. Kouyoumjian, P.H. Pathak, and W.D. Burnside, "A Uniform GTD for the Diffraction by Edges, Vertices, and Convex Surfaces," Acoustic, Electromagnetic and Elastic Wave Scattering-Focus on the T-Matrix Approach, V.K. Varadan, V.V. Varadan, Eds., New York: Pergamon Press,1980, pp. 373-397.

5. W.D. Burnside and P.H. Pathak, "A Corner Diffraction Coefficient," to be published.

6. E.L. Pelton, and W.D. Burnside, "Edge Diffraction Point Analysis used in Near-Field On-Aircraft Antenna Studies," The Ohio State University ElectroScience Lab., Dept. of Electrical Engineering; prepared under Contract N00019-77-C-0299 for the Naval Air Systems Command, Report 784685-2, October 1977.


DAT
FILM